Deformation and Strength of Engineering Ceramics and Single Crystals

G. A. Gogotsi & D. Yu. Ostrovoy

Institute for Problems of Strength, National Academy of Sciences of Ukraine, 2 Timiryazevskaya str., Kiev 252014, Ukraine

Abstract

A comparative investigation has been performed of the laws of deformation and strength of engineering silicon nitride-, alumina, and zirconia-based ceramics, as well as zirconia crystals. The specimens were tested in four-point bending in air over a temperature range from ambient to 1400°C. The materials' mechanical behaviour was analyzed by load versus deflection diagrams (deformation diagrams). It has been found that above the brittle-to-ductile transition temperature, T_{BD}, for the ceramics studied it is possible to choose such combinations of temperature and deformation rate, which would ensure the same path of deformation diagrams, i.e. equivalent influence of those two parameters on the mechanical behaviour of ceramics is observed. The mechanism of inelastic deformation of the ceramics studied is shown to be associated with the development of two processes: viscous flow of the grain boundary phase and crack propagation to a critical size, with one of them prevailing at different load levels. In contrast to ceramics, the strength of zirconia crystals remained practically unchanged (partially-stabilized crystals) up to 1400°C or even increased (fully-stabilized crystals). For all the crystals, static elasticity moduli were independent of the number of repeated-static loading cycles at high temperatures (their values remained constant), while for ceramics a reduction was observed. Partially-stabilized zirconia crystals, as compared to other investigated materials, exhibited practically no creep up to 1400°C at loads close to limiting ones. This allows them to be considered as a promising engineering material for high-temperature application.

1 Introduction

Along with extensive investigations of engineering ceramics and their application in industry, nowadays researchers pay much attention to finding possibilities for practical application of such promising refractory materials as zirconia crystals.[1] According to some preliminary estimates[2-5] in a high-temperature loading region they can compete not only with metals but also with ceramics. One of the reasons restricting the introduction of these materials in many areas of engineering is insufficient understanding of specific features of their mechanical behaviour at high temperatures. This is associated with the fact that most studies, e.g. of zirconia crystals, are concerned with physical aspects of their deformation and fracture[6-15] and the data on their strength and fracture toughness which appear in some publications[2,4,16,17] are insufficient for the correct evaluation of their performance from the criteria used in practical engineering. This situation with both ceramics and single crystals can be explained by the use of different test methods that result in inconsistency of the results obtained. In this case, for instance, strength characteristics of such materials determined in the high-temperature region by the known standards[18] at one constant loading or deformation rate turn out to be insufficient for revealing a complete picture of their actual mechanical behaviour. This conclusion is strongly confirmed by the fact[19] known for conventional structural materials (metals, polymers), according to which appreciable changes occur in the conditions of reaching the ultimate state by them due to simultaneous temperature and loading or deformation rate variation. In this case the probability of their brittle fracture even at the temperature of viscous (plastic) flow[20] may increase. The data on this problem for ceramics[22-25] and single crystals[2,8,21] are not only limited but in most cases[21,23,25] they do not take into account such an important characteristic of the materials as their deformability. For this reason such results tell us little of possible performance of these materials under real service conditions. To eliminate this gap the present work was performed where attention was paid to the investigation of the laws of deformation and strength of zirconia crystals at different temperatures and deformation rates as compared with the

Table 1. Physico-mechanical characteristics of investigated ceramics and crystals at ambient temperature (average values)

Material (orientation of the specimen axis)	Density (g/cm^3)	Ultrasonic velocity (m/s)	Elastic modulus (GPa)		Bending strength $(MOR)^a$ (MPa)	Ultimate strain^a $(\times 10^{-4}\ m/m)$
			Dynamic	Static^a		
Ceramics						
SN-1	3·21	9289	277	280	465	16·6
SN-2a	3·27	9690	307	305	510	16·7
A-1	3·70	9347	323	320	300	9·4
Y-PSZ-3	5·94	5951	210	207	908	44·0
Crystals						
Y-FSZC-10 (<101>)	5·87	5933	207	180	134	7·4
Y-FSZC-20 (<101>)	5·76	6116	215	185	140	7·6
Y-PSZC-3 (<111>)	6·04	5394	176	149	642	43·0

^{a}Obtained at V_{ch} = 0·5 mm/min.

behaviour of the most widely spread types of engineering ceramics (silicon nitride, alumina, zirconia) under similar loading conditions.

2 Materials and Experimental Procedure

The materials investigated were silicon nitride-, alumina-, and zirconia-based ceramics and zirconia crystals (Table 1).

A silicon nitride-based ceramic, SN-1,[26] with an addition in the initial state of 5% Y_2O_3 and 2% Al_2O_3 was produced by hot-pressing in graphite moulds (the sintering temperature was 1750°C, pressure 50 MPa). Its main components were β-Si_3N_4 and a grain boundary phase. The latter consisted of the amorphous phase containing Si, N, Al, Y, O and yttrium oxynitrides. The SN-1 structure was a mixture of equiaxial and elongated grains of β-Si_3N_4. The average size of those grains was 3–5 μm. A silicon nitride-based ceramic, SN-2,[26] was obtained from powders: 82% Si, 2·5% Al_2O_3 and R_2O_3 (a mixture of rare-earth element oxides: 64% Nd_2O_3, 17% Pr_2O_3, 14% La_2O_3 and 1% Sm_2O_3) by the method of reaction bonding (nitriding in an atmosphere of N_2 + H_2 at 1380°C). Then it was sintered under pressure of 50 MPa at 1850°C in an atmosphere of N_2. This ceramic consisted mostly of β-Si_3N_4 and of the grain boundary phase. By varying the quantity of R_2O_3 three compositions of this ceramic were obtained: SN-2a, SN-2b and SN-2c with the content of the amorphous phase 8·5, 10·6 and 13·5%, respectively. In its structure SN-2 ceramic was close to SN-1. The cross dimension and the length of elongated grains β-Si_3N_4 of this ceramic were, on the average, 0·5 and 4 μm, respectively.

An alumina-based ceramic, A-1,[26] with an addition of MgO was produced by semi-dry pressing at a

pressure of 200 MPa and sintered in air at 1600°C. Its grain size averaged between 4 μm and 5 μm.

Zirconia-based materials contained different quantities of stabilizing additive Y_2O_3. Thus Y-PSZ-3 ceramic with 3 mol% of Y_2O_3 was hot-pressed at 1750°C in an atmosphere of N_2. It contained a minute quantity of Al_2O_3. Its average grain size was less than 1 μm. Crystals[3,27] were grown by a skull melting technique using direct high-frequency heating. Their growth rate was 10 mm/h. They were then cooled down from the temperature of their crystallization at a rate of 10°C/min. The crystals contained 3(Y-PSZC-3), 10(Y-FSZC-10) and 20(Y-FSZC-20) mol% of Y_2O_3. The first of them were partially stabilized, the rest were fully stabilized. In accordance with the classification,[28] all the materials chosen for the investigation were brittle (i.e. deforming linearly-elastically at ambient temperature).

The tests in the temperature range from ambient to 1400°C were performed in air using the loading module (Fig. 1) designed and manufactured for the purpose and mounted on a conventional testing machine. The test method has been evaluated elsewhere.[5,28] The test specimens were beams 3·5 × 5·0 × 50·0 mm in size cut from billets by a diamond tool and then ground along the longitudinal axis. Their sharp edges were bevelled. Crystallographic orientation of the crystal specimen longitudinal axes was defined by the Laue back-reflection X-ray technique. Prior to mechanical testing, dynamic elasticity moduli E_d were determined from measurements of the ultrasonic vibration propagation velocity along the specimen longitudinal axis.

The specimens were loaded in four-point bending under isothermal conditions with the testing machine cross-head speed, V_{ch} from 0·005 to 5·0 mm/min. As most often happens in these investi-

(a)

Fig. 2. Histogram of the testing machine cross-head speeds, V_{ch} (from the data from 175 literature sources): (1) the main speed.
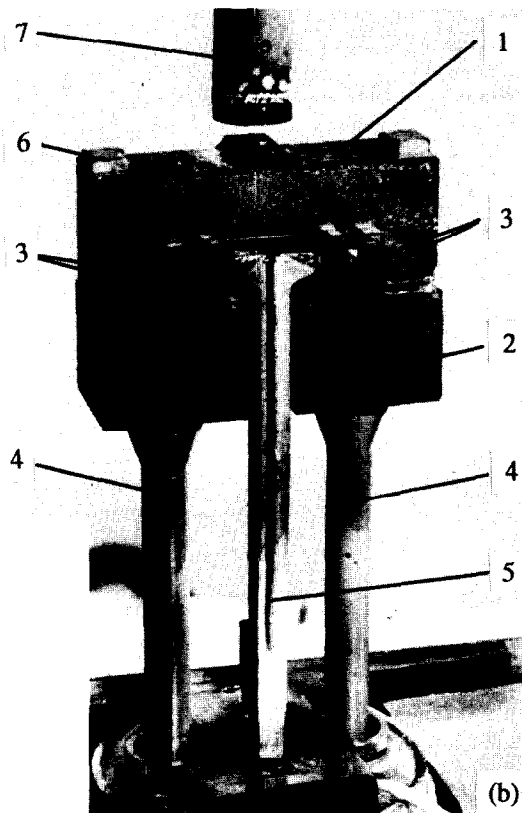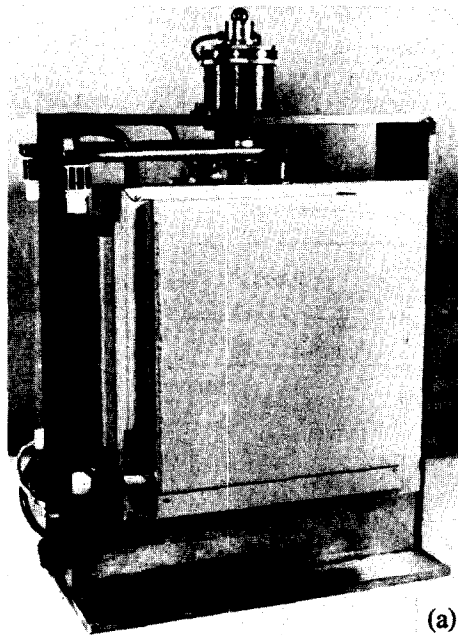

(b)

Fig. 1. General view of (a) the loading module and (b) the loading arrangement. (1) Upper prism, (2) lower prism, (3) swing roller support, (4) supporting column, (5) bending deflection measurer, (6) slide-way, (7) loading rod.

gations (Fig. 2), the cross-head speed V_{ch} equal to 0·5 mm/min was chosen as the main one. It is convenient because the time to specimen fracture in testing is less than 1 min. The distance between the inner and outer swing roller supports was 20 and 40 mm, respectively. A special feature of the experimental procedure used was recording 'applied load–specimen deflection' dependences (the deformation diagrams) using a deflection measuring
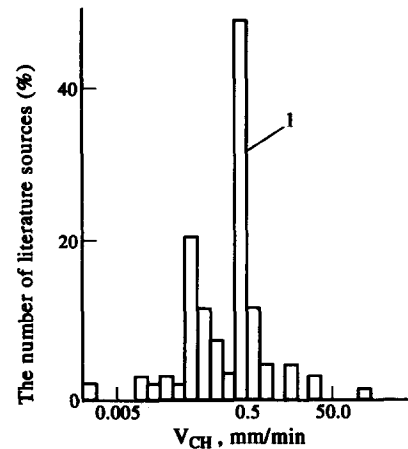
gauge (LVDT)[29] which was hung on the specimen (5 in Fig. 1) and was in no way connected to the testing machine. In this way the influence of deformation of the loading device parts was excluded from the measurements, unlike conventional determination of specimen deflection by the testing machine cross-head displacement or by the measuring gauge connected with the testing arrangement.

Mechanical characteristics were calculated by the known relationships of applied mechanics (linear-elastic approximation), i.e. strength, for instance, was characterized by the magnitude of the modulus of rupture (MOR $= 2aP/bh^2$, where P is the load, α is the length of the cantilever part of the specimen, b and h are the specimen width and height, respectively). This approach proved to be acceptable since the present work involved a comparative analysis of the mechanical behaviour of ceramics and crystals rather than precise determination of their strength characteristics. At the same time, the known Nadai formula ($\sigma = 2a/bh^2 \times (P + \delta/2 \cdot dP.d\delta)$, where σ is the mean stress in the specimen, δ is the specimen deflection) used earlier by us[3,29] and other investigators[22] turned out to be unacceptable here, since the deformation diagrams of the specimens (see below) had not only ascending but also extensive horizontal portions.

3 Results

The main investigations were performed at temperatures above some critical temperature for each of the materials at which their deformation diagrams exhibited nonlinearity, associated with the intensification of creep. At the same time, the dependence of the mechanical properties of these materials on time or strain rate was observed. The latter was defined by the cross-head speed, V_{ch}.
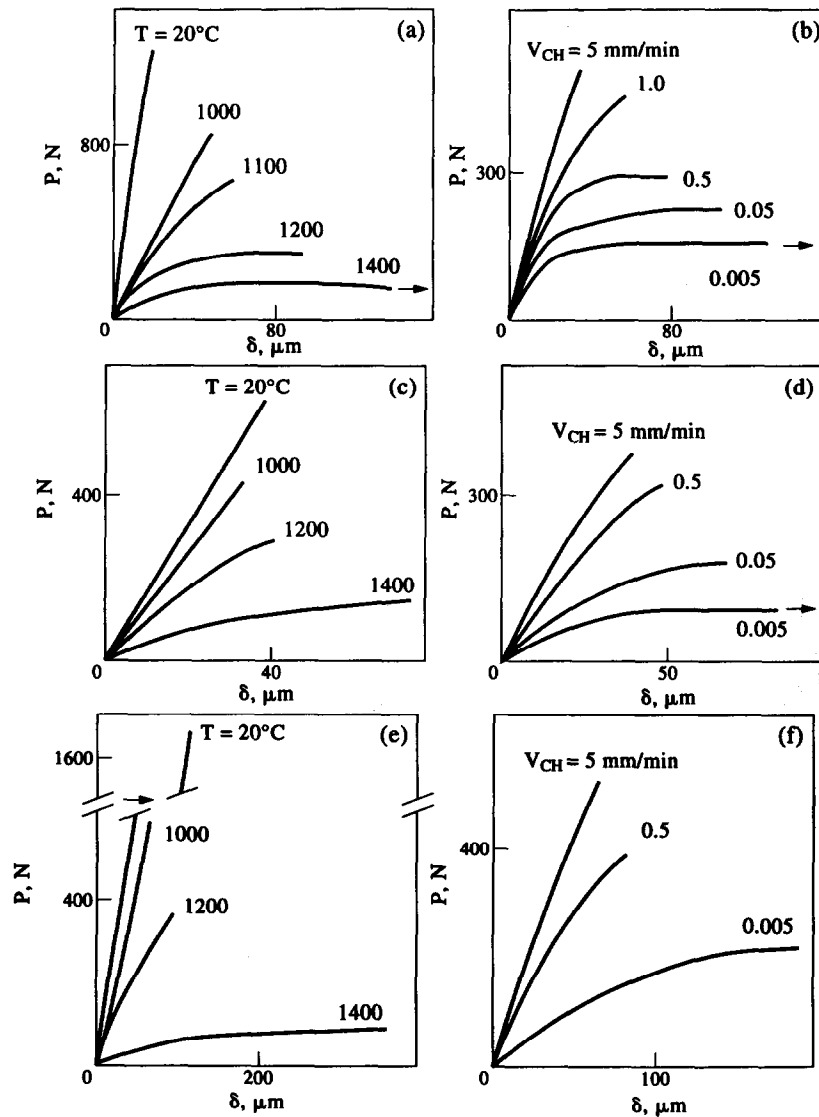
Fig. 3. The influence of the temperature, T (a,c,e) at V_{ch} = 0·5 mm/min and of the speed V_{ch} (b,d,f) at T = 1200°C on the appearance of the load (P) versus deflection (δ) diagrams: (a,b) SN-1; (c,d) A-1; (e,f) Y-PSZ-3.

This critical temperature is often called brittle-to-ductile transition temperature, T_{BD},[22,23] by analogy with the respective transition in steels. Note that the T_{BD} value is not a material constant: it depends on the strain rate, the size of the specimens, their structure, etc. In the present work, T_{BD} was determined by the deviation from linearity of the deformation diagrams for the same specimens of

the materials studied, recorded while the temperature was increasing gradually and at a cross-head speed of 0·5 mm/min. For SN-1, SN-2 and A-1 ceramics the T_{BD} value was about 1100–1150°C and for Y-PSZ-3 it was about 1050°C. For zirconia crystals T_{BD} was in the range 1000–1100°C, whereas it was 500–600°C when the latter were loaded by the Vickers indenter.[30]
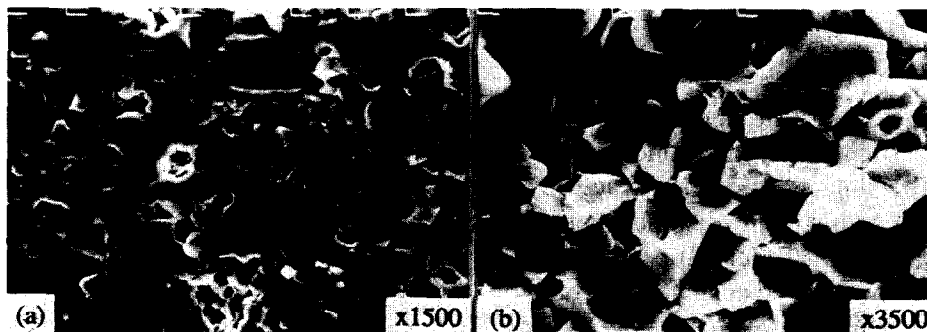

Fig. 4. Photographs of fracture surface fragments of A-1 specimens tested at T = 1200°C and (a) V_{ch} = 5·0 and (b) V_{ch} = 0·005 mm/min.
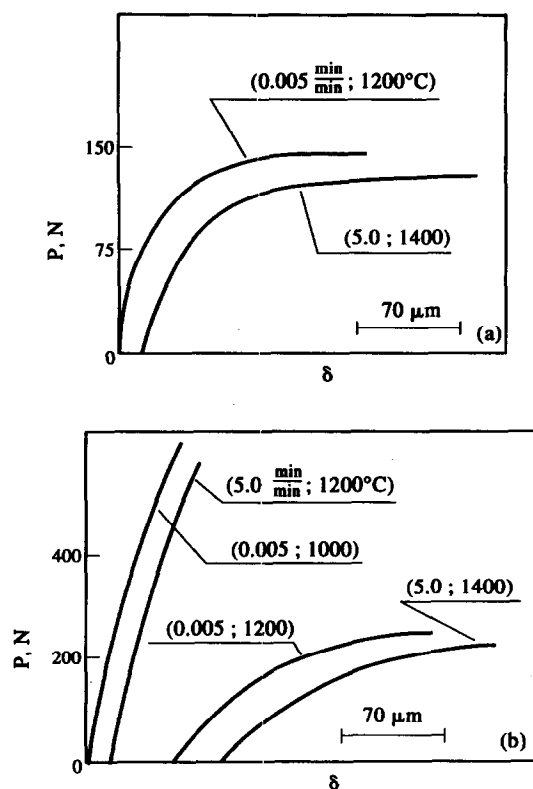
Fig. 5. Load (P) versus deflection (δ) diagrams for (a) SN-1 and (b) Y-PSZ-3 under different conditions of deformation (V_{ch} in mm/min; T in °C).

Check tests of ceramics at temperatures below T_{BD} revealed that, irrespective of the combination of temperature and cross-head speed, it exhibited linearly-elastic deformation and brittle fracture thus confirming the results obtained earlier.[22-24] In particular, the cross-head speed affected the strength of only alumina-based ceramics A-1. Such an influence is generally evaluated by the magnitude of the power parameter N in the equation[25] for the crack growth rate (V) in a corrosion-active environment: $V = M \cdot K_I^N$, where M is a parameter, K_I is the stress intensity factor at the crack tip. The higher the value of N, the greater the material resistance to the subcritical crack growth. The value of N was determined from the equation $\sigma_1/\sigma_2 = (V_{ch_1}/V_{ch_2})^{1/N+1}$, where σ_1 and σ_2 are fracture stresses (MOR) at speeds V_{ch_1} and V_{ch_2}, respectively, which was obtained from analytical relationships proposed elsewhere.[25] In the case for A-1 the magnitude of N was 20, whereas for the test of ceramic materials it exceeded 100. It should be noted that the above N values for ceramics remained almost unchanged up to the T_{BD} temperature, above which their reduction was observed.

The deformation diagrams obtained for ceramics at temperatures above T_{BD} revealed that irrespective of the production technology (see the test results for other similar materials[27,29]) their mechanical behaviour at increasing temperature, T, and constant V_{ch} (Fig. 3(a),(c),(e)) is similar to that

at decreasing V_{ch} and constant T (Fig. 3(b),(d),(f)). In addition, at a certain combination of the temperature and speed, the ceramics exhibited (see Fig. 3) a transition from totally inelastic to linearly-elastic deformation and brittle fracture even at the temperatures of probable material creep. This was also evidenced by specific features of ceramic specimen fracture surfaces, where (e.g. material A-1) the transition from primarily intercrystalline (Fig. 4(b)) to mostly transcrystalline (Fig. 4(a)) crack propagation was observed with an increase in V_{ch}. This fact was also noted by other investigators.[31]

These data allow us to say that, at least in the temperature and V_{ch} ranges used, an equivalence of the influence of these two parameters on the resistance of ceramics to deformation took place, since different pairs of deformation conditions were selected (V_{ch_i}, T_i). This ensured similar paths of the deformation diagrams within the scatter band of the experimental data, as is shown, for instance, in Fig. 5 for SN-1 and Y-PSZ-3 materials. It should be noted that these equivalent conditions of deformation also result in similar features of micro- and macrofractures of specimens of the given ceramics.

An interesting feature of the ceramic behaviour also reported elsewhere[22] was the appearance of characteristic horizontal portions (Fig. 3) on the deformation diagrams at temperatures above T_{BD} and at low V_{ch} values, where the increase in specimen deformation occurred at almost constant applied load. To find out the reasons for the appearance of such portions, as an example, a detailed investigation was carried out on SN-1 specimens only, since the behaviour of all the ceramics was similar. After testing, a lot of cracks (Fig. 6(a)) appeared on the specimen surface at the sites of action of the maximum tensile stresses σ_t. Their faces were mostly orthogonal to the direction of those stresses. On fracture surfaces there were ridged regions (Fig. 6(b)) corresponding to those cracks and their size grew with both a decrease in V_{ch} at constant temperature, and with an increase in temperature at constant V_{ch}. At sufficiently low temperature (below T_{BD}) and at high V_{ch} these regions on fracture surfaces were almost indistinguishable with a conventional optical microscope. We should note that all the observations for SN-1 materials were also true of A-1. With Y-PSZ-3 materials the size of these regions, as well as that of the cracks (Fig. 6(c)) was appreciably smaller than with other ceramics investigated under the same loading conditions (V_{ch_i}, T_i) (Fig. 5).

For this reason it could be expected that those cracks affected appreciably the mechanical properties at high temperatures. For SN-1 materials this influence was observed under repeated-static load-
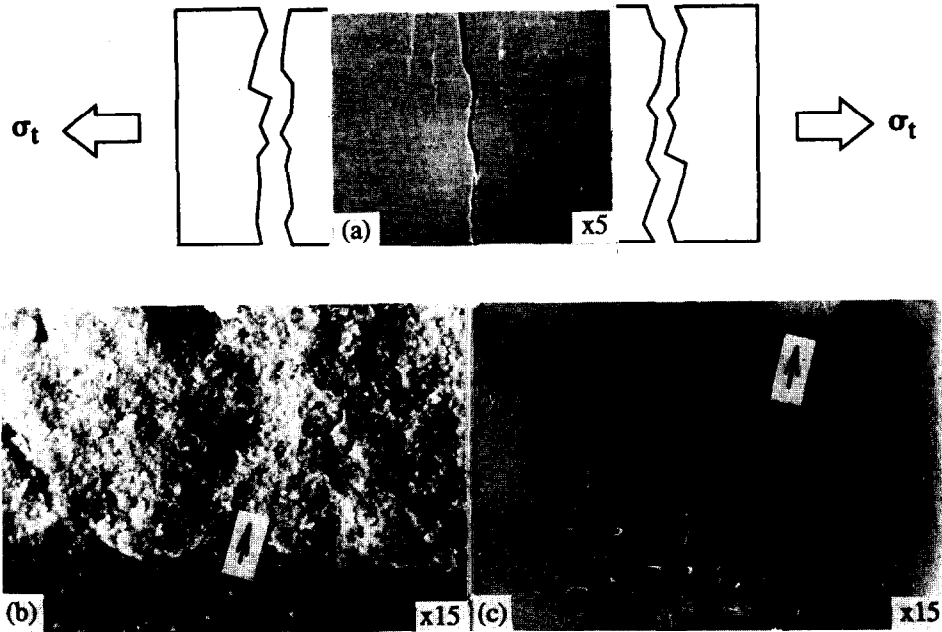
Fig. 6. Photographs of (a) tensile and (b) fracture surface of SN-1 and (c) fracture surface of Y-PSZ-3 specimens tested at T = 1200°C and V_{ch} = 0·005 mm/min. Arrows (b,c) show surface roughness.

ing (Fig. 7(a)) and in creep tests (Fig. 8(a)). Under such loading conditions the process of crack growth was strongly intensified each time when the applied load reached the magnitudes corresponding to the horizontal portions on the deformation diagrams. For this ceramic with each loading cycle the slopes (α) of the lines tangent to the diagram (Fig. 7(a)) at the origin of the coordinates decreased. The slope of the diagram is related to the elasticity modulus, E, by a simple expression $tg\alpha$ = $Eb/2(h/a)^3 M_p/M_\delta$, where M_p and M_δ are the scales

of the plot in Fig. 7(a) along the axes 'p' and 'δ', respectively. See above for other designations. The creep stage associated with such crack formation and culminating in fracture manifested itself more distinctly (Fig. 8(a)) only at loads close to the limiting ones on the deformation diagrams. At the same time, the Y-PSZ-3 material exhibited no noticeable reduction of static elasticity modulus (Fig. 7(b)) under repeated-static loading, and in creep testing no creep stage (Fig. 8(b)) characteristic of the crack propagation in SN-1 was observed due to consider-
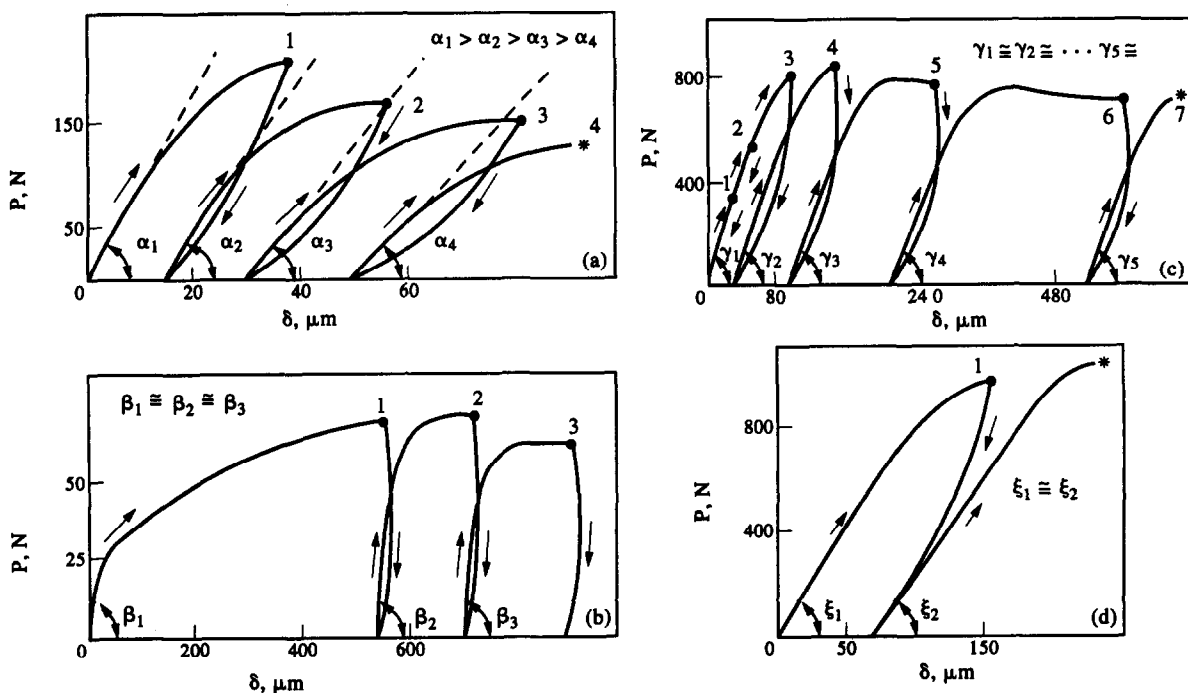

Fig. 7. Unloading and repeated loading diagrams for (a) SN-1 at V_{ch} = 0·05 mm/min and 1200°C; (b) Y-PSZ-3 at 0·5 mm/min and 1300°C; (c) Y-FSZC-10 at 0·5 mm/min and 1400°C; (d) Y-PSZC-3 at 0·005 mm/min and 1400°C. The number of repeated static load applications (1–7), the beginning of unloading (●), specimen fracture (*).
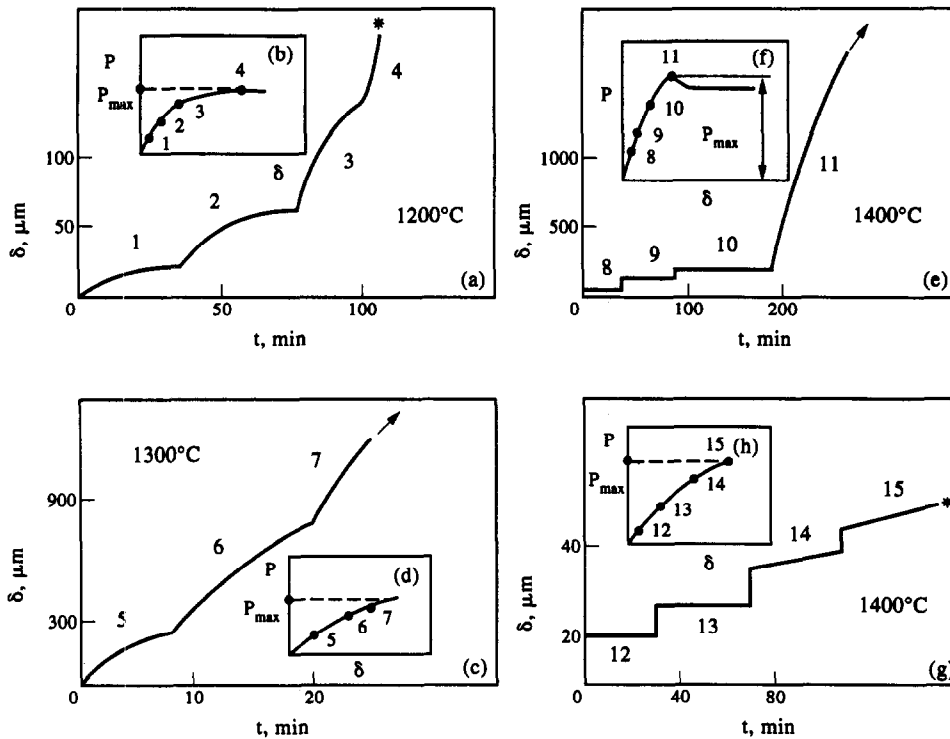
Fig. 8. Creep curves for (a) SN-1, (c) Y-PSZ-3, (e) Y-FSZC-10 and (g) Y-PSZC-3 at P = const. P_{max} = 200 (b,d), 600 (f) and 900 (h) N: 30 (1,5,8,12), 50 (2,6,9,13), 70 (3,7,10,14) and 100 (4,11,15) %P_{max}. Specimen fracture (*).

able residual deformation of specimens which does not result in their fracture. Thus, crack propagation was probably one of the reasons for the increase in nonlinearity of the ceramics deformation diagrams, though with Y-PSZ-3 material, where the crack growth is less pronounced, such behaviour could be induced for other reasons as well.

Nonlinearity of the deformation diagrams and crack propagation could also occur in ceramics at high (above T_{BD}) temperatures as a result of softening of its grain boundary phase which has a lower melting temperature than the basic material. In order to confirm this an evaluation (Fig. 9) was made of the influence of the quantity of glass

Fig. 9. The influence of the quantity of additives on the MOR (1–4) for SN-2: T = 20°C (1,2), 1200°C (3,4). V_{ch} = 0·5 (1,3) and 0·005 (2,4) mm/min.

phase upon the mechanical behaviour of the SN-2 material which is similar in its properties to SN-1 but contains different quantities of amorphous additives (composition SN-2a, S-2b and SN-2c). It was found that with such combination of the temperature and speed, which provides a near linear-elastic deformation of the SN-2 material (Fig. 10(a)), an increase in the quantity of additives resulted in the increase in its strength (1–3, in Fig. 9), while at inelastic deformation it caused a decrease in strength (4 in Fig. 9), intensification of creep (Fig. 10(b)), enhancement of the crack growth process and an increase in nonlinearity (Fig. 10(a)) of the deformation diagrams.

Zirconia crystals were studied at minimal (ambient) and maximal (1400°C) test temperatures. At ambient temperature all crystals (similarly to the ceramics studied) exhibited linear-elastic deformation (1 in Fig. 11(a) for Y-FSZC-10). At 1400°C Y-FSZC crystal exhibited an increase in strength as compared to that at ambient temperature (Table 2) at all the speeds used in the experiment (see also Refs 2 and 3).

At 1400°C, when Y-FSZC-10 crystals were tested at high V_{ch}, their deformation diagrams were linear, similar to those at ambient temperature (2 in Fig. 11(a)). At V_{ch} = 0·5 mm/min their diagrams showed horizontal portions (3 in Fig. 11(a)), at V_{ch} ≤ 0·05 mm/min well-pronounced upper and lower yield points were observed (4, 5 in Fig. 11(a)). Note that similar deformation behaviour at 1400°C was observed for Y-FSZC-20 crystals as
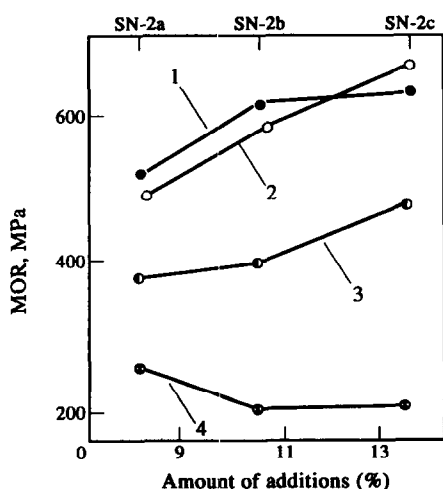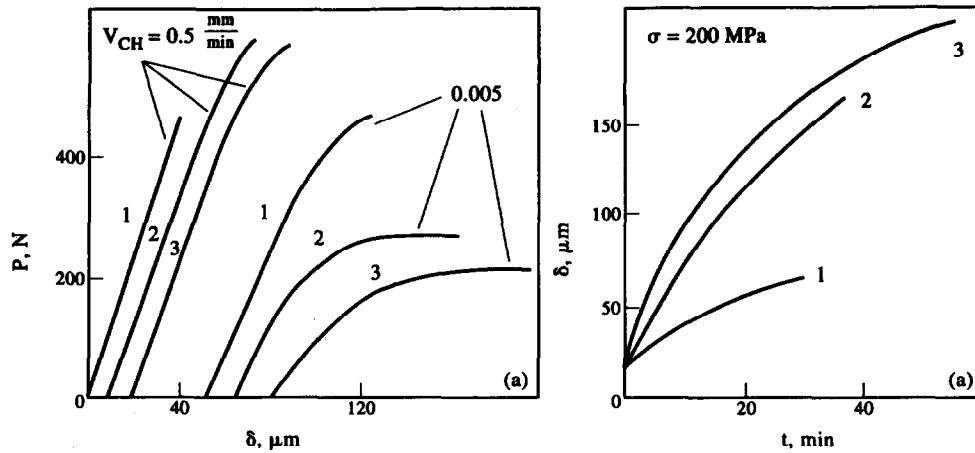
Fig. 10. The influence of the quantity of additives on (a) the load (P) versus deflection (δ) diagrams and (b) creep curves at $T =$ 1200°C for: SN-2a (1), SN-2b (2), SN-3c (3).

well. However, the diagrams of the latter were already linear at $V_{ch} = 0.5$ mm/min and the ratio of the upper and lower yield points increased almost twice at $V_{ch} = 0.005$ mm/min as compared to those shown in Fig. 11(a). An interesting observation is that the appearance of the upper and lower yield points for all Y-FSZC crystals was preceded by characteristic maximum in strength (see 3 in Fig. 11(a)).

Y-FSZC crystal samples tested at 1400°C and at speeds equal to or above 0·5 mm/min fractured into many pieces both transverse to and along their axis (see Ref. 27 for details). In contrast, specimens tested at lower speeds (0·05 and 0·005 mm/min) were curved strongly without fracturing, the fact being also noted for similar materials.[2]

With partially stabilized Y-PSZC-3 crystals, whose strength remained practically unchanged (Table 2) up to 1400°C, there were practically no inelastic strains (Fig. 11(b)) and they appeared only at the loads close to the limiting ones irrespective of the temperature and speed regimes. In fracture the specimens of these crystals separated generally into several parts, yet no traces of residual strains were observed in them even at $V_{ch} = 0.005$

mm/min. We should note that ceramic specimens at all the loading regimes used fractured with only one propagating crack (Fig. 6(a)) though at high temperatures very many nuclei of other cracks could be observed next to it.

4 Discussion

The data presented above may be an indication of a noticeable difference in specific features of the mechanical behaviour of the ceramics and zirconia single crystals investigated.

A specific feature of the ceramic behaviour (as was also noted in Refs 32 and 33) is the deterioration of its strength characteristics at temperatures above T_{BD}. As has been confirmed by the results of the present investigation, this is to a great extent associated with the crack propagation in ceramics (see Fig. 6) In oxygen-free materials such defects can also originate due to oxidation.[34] The development of these defects changes appreciably the inelastic behaviour of ceramics whose specific feature is the presence of extensive horizontal portions (Fig. 3) on the deformation diagrams
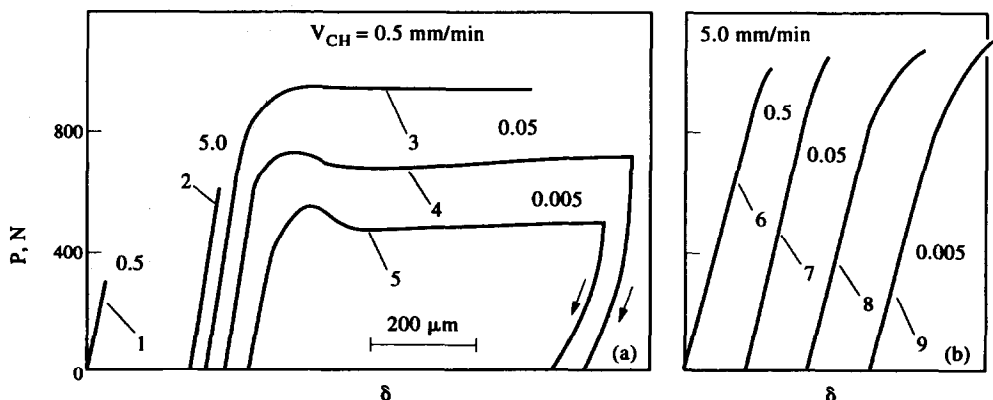

Fig. 11. Load (P) versus deflection (δ) diagrams for (a) Y-FSZC-10 and (b) Y-PSZC-3 at $V_{ch} =$ var.: $T =$ 20°C (1) and 1400°C (2–9). Arrows show specimen unloading.

Table 2. Average values of mechanical characteristics of investigated crystals at 1400°C

Material	V_{ch} (mm/min)	Elastic limit (MPa)	Upper yield point[a] (MPa)	Lower yield point (MPa)	Strain at elastic limit ($\times 10^{-4}$ m/m)	Strain[a] at upper yield point (MPa)	Elastic modulus (GPa)
Y-FSZC-10	5·0	274	—	—	17·5	—	157
	0·5	327	445	445	23·2	51·5	141
	0·05	269	338	318	18·7	32·2	144
	0·005	210	250	234	16·9	28·4	124
Y-FSZC-20	5·0	213	—	—	15·3	—	140
	0·5	300	—	—	21·6	—	139
	0·005	276	324	295	23·2	35·7	119
Y-PSZC-3	5·0	393	444	—	31·2	37·5	126
	0·5	403	475	—	33·0	42·5	122
	0·05	400	550	—	32·8	75·2	122
	0·005	390	556	—	35·8	74·4	109

[a]For Y-PSZC-3 crystals — ultimate stress and strain values.

recorded at a constant speed, corresponding approximately to the load (or stress) which induces a continuous increase in the strain rate at the final stage of creep (Fig. 8(a)), while, for instance in metals this effect is often associated[35] with steady-state creep stage where, as is known, the strain rate is constant.

Thus, the data obtained reveal that the general mechanism of ceramic inelastic deformation, at least for the silicon nitride- and alumina-based materials studied in this investigation, can consist of two simultaneous and competing effects: softening and viscous flow of the grain boundary phase (which has been emphasized in a number of investigations[36-38]) and the growth of cracks up to their critical size. In this case the first effect prevails at low load levels and the second becomes appreciable with the load reaching its limiting value, as can be seen in Fig. 8 from the transition, at stepwise load increase, from the stage of transient creep to that associated with cracking. If we consider zirconia-based materials, for Y-PSZ-3 ceramics the results obtained (Figs 7(b) and 8(c)) point to the existence of most likely one and the same mechanism of deformation (creep) which is not connected with noticeable upsetting of the material continuity.

For fully stabilized (cubic) zirconia crystals Y-FSZC a noticeable increase in their strength with temperature is a distinguishing feature in their behaviour compared to ceramics. One of the causes of this strength enhancement can be the annealing of specimens in the course of testing and the resulting reduction of the degree of their surface damage caused by machining. Indirect evidence for the above assumption is the fact that the ambient temperature testing of specimens annealed at 1400°C yielded the following results: the strength of specimens which were not annealed was 135 and 145 MPa and that of annealed ones 170 and 215 MPa

for Y-FSZC-10 and Y-FSZC-20, respectively. A similar conclusion was also made elsewhere.[2]

An increase in the difference between the upper and lower yield points of Y-FSZC-20 crystals is probably associated with the formation of a more ordered solid solution ZrO_2-Y_2O_3[6,8] with an increase in the content of Y_2O_3 from 10 to 20%, while the appearance of two yield points in such crystals is related by some authors[6,8,11] to the involvement of additional slip systems in their deformation process. This can be evidenced by a noticeable intensification of creep in Y-FSZC crystals (Fig. 8(c)) only when the load reaches the upper yield point, whereas in ceramics it was registered at practically all load levels.

The maximum in the Y-FSZC crystal strength prior to the appearance of the upper and lower yield points has not been explained adequately in the present paper, though the effect of strength increase prior to the appearance of plasticity or creep is also known for ceramics.[23]

The deformation diagrams of Y-FSZC and Y-PSZC-3 crystals at all temperature and speed combinations used in the experiment exhibit pronounced linear portions (Fig. 11) within which the deflection disappears completely (Fig. 7(c),(d)) after removal of the applied load. With ceramics such portions on the diagrams were observed only at low temperatures (close to T_{BD} and lower) or at high speeds. It is probably owing to this fact, as well as to the absence of grain boundaries, that elastic moduli of Y-FSZC and Y-PSZC-3 crystals in contrast to ceramics were independent (Fig. 7(c),(d)) of the number of cycles of repeated loading irrespective of the limiting values of the loads reached, which correspond to the appearance of plateaus on the deformation diagrams with the former crystals and to fracture with the latter. The Y-PSZC-3 crystals under repeated loading exhibited an increase in the proportionality limit (Fig. 7(d)), though similarly for ceramics and

Y-FSZC crystals the unloading lines are indicative of their viscoelastic behaviour.

The existence in practice of equivalent ceramic deformation regimes (Fig. 5) can be probably explained by the action under such loading conditions of the same predominant deformation mechanism which is independent of the load and strain level. There was no possibility of choosing such deformation regimes for crystals, probably owing to differences in the character of their deformation (Fig. 8(e),(g)) at different loads.

As noted above, with all the ceramics and Y-FSZC crystals studied, creep intensified noticeably at the limiting loads, while with Y-PSZC-3 crystals almost complete absence of creep (Fig. 8(g)) was observed. This once again testifies to their appreciable difference from and the advantage over all other materials studied.

5 Conclusions

In the present investigation an attempt was made to obtain a general comparative picture of the mechanical behaviour of different types of ceramics and zirconia single crystals over a wide range of temperatures and deformation rates.

Specific features of the behaviour of the materials studied supplement appreciably the information about the processes which accompany their deformation and fracture and show that when making a choice among them for high temperature applications using, as most often happens in engineering practice, conventional criteria of applied mechanics, for a reliable evaluation of their load carrying capacity and, on the whole, efficiency, one should take into account their actual mechanical properties rather than idealize them using different hypotheses.

In spite of the fact that the deformation and fracture mechanisms of partially stabilized zirconia crystals have not been studied sufficiently, comparison of their mechanical properties with those of ceramics under different loading conditions reveals their higher serviceability at higher (up to 1400°C) temperatures. This makes it possible to consider them as new promising engineering materials.

References

1. Ingel, R., Lewis, D., Bender, B. A. & Rice, R. W., Physical, microstructural and thermomechanical properties of ZrO_2 single crystals. *J. Amer. Ceram. Soc.*, **26** (1984) 408–14.
2. Ingel, R., Lewis, D., Bender, B. A. & Rice, R. W., Temperature dependence of strength and fracture toughness of ZrO_2 single crystals. *J. Amer. Ceram. Soc.*, **65** (1982) 150–2.
3. Gogotsi, G. A., Lomonova, E. E. & Osiko, V. V., Studies of mechanical characteristics of zirconia single crystals for structural application. *Refractories*, **32** (1991) 14–17.
4. Gogotsi, G. A., Drozdov, A. V. & Pejchev, V. G., Mechanical behavior of zirconium dioxide crystals partially stabilized with yttrium oxide. *Strength of Materials*, **23** (1991) 86–91.
5. Gogotsi, G. A., Lomonova, E. E. & Pejchev, V. G., Strength and fracture toughness of zirconia crystals. *J. Eur. Ceram. Soc.*, **11** (1993) 123–32.
6. Dominguez-Rodriguez, A., Lagerlof, K. P. D. & Heuer, A. H., Plastic deformation and solid-solution hardening of Y_2O_3-stabilized ZrO_2 *J. Amer. Ceram. Soc.*, **69** (1986) 218–84.
7. Dominguez-Rodriguez, A., Lanteri, V. & Heuer, A. H., High-temperature precipitation hardening of two-phase Y_2O_3-partially-stabilized ZrO_2 single crystals. The first report. *J. Amer. Ceram. Soc.*, **69** (1986) 285–7.
8. Lankford, J., Page, R. A. & Rabenberg, L., Deformation mechanisms in yttria-stabilized zirconia. *J. Mater. Sci.*, **23** (1988) 4144–56.
9. Heuer, A. H., Lanteri, V. & Dominguez-Rodriguez, A., High-temperature precipitation hardening of Y_2O_3-partially-stabilized ZrO_2 (Y-PSZ) single crystals. *Acta Metall.*, **37** (1989) 559–67.
10. Martinez-Fernandez, J., Jimenez-Melendo, M., Dominguez-Rodriguez, A. & Heuer, A. H., High-temperature creep of yttria-stabilized zirconia single crystals. *J. Amer. Ceram. Soc.*, **73** (1990) 2452–56.
11. Fries, E., Guiberteau, F., Dominguez-Rodriguez, A., Cheong, D.-S. & Heuer, A. H., High-temperature plastic deformation of Y_2O_3-stabilized ZrO_2 single crystals. I. The origin of the yield drop and associated glide polygonization. *Phil. Mag. A.*, **60** (1989) 107–21.
12. Cheong, D.-S., Dominguez-Rodriguez, A. & Heuer, A. H., High-temperature plastic deformation of Y_2O_3-stabilized ZrO_2 single crystals. II. Electron microscopy studies of dislocation substructures. *Phil. Mag. A.*, **60** (1989) 123–38.
13. Cheong, D.-S., Dominguez-Rodriguez, A. & Heuer, A. H., High-temperature plastic deformation of Y_2O_3-stabilized ZrO_2 single crystals. III. Variation in work hardening between 1200 and 1500°C. *Phil. Mag. A.*, **63** (1991) 377–88.
14. Dominguez-Rodriguez, A., Cheong, D.-S. & Heuer, A. H., High-temperature plastic deformation of Y_2O_3-stabilized ZrO_2 single crystals. IV. The secondary slip systems. *Phil. Mag. A.*, **64** (1991) 923–29.
15. Michel, D., Mazerrolles, L. & Gorban, M., Fracture of metastable tetragonal zirconia crystals. *J. Mater. Sci.*, **18** (1983) 26–8.
16. Ingel, R. P. & Rice, R. W., Room-temperature strength and fracture of ZrO_2-Y_2O_3 single crystals. *J. Amer. Ceram. Soc.*, **65** (1982) 108–9.

17. Pajares, A., Guiberteau, F., Dominguez-Rodriguez, A. & Heuer, A. H., Microhardness and fracture toughness anisotropy in cubic zirconium oxide single crystals. *J. Amer. Ceram. Soc.*, **71** (1988) 332–3.

18. Quinn, G. D. & Baratta, F. I., Flexure data. Can it be used for ceramics part design? *Adv. Mater. Proc.*, **1** (1985) 31–5.

19. Sukhovarov, V. F., On the equivalence of the temperature and strain rate influence on the curves of copper and nickel plastic flow. *Izvestiya vuzov, Fizika*, **5** (1959) 164–71 (in Russian).

20. Bartenev, G. M., Strength and fracture mechanisms of polymers. Khimiya, Moscow, 1984 (in Russian).

21. Lankford, J., Inverse strain rate effects and microplasticity in zirconia crystals. *J. Mater. Sci. Lett.*, **8** (1989) 947–9.

22. Cannon, R. F., Roberts, J. T. A. & Beals, R. J., Deformation of UO_2 at high temperatures. *J. Amer. Ceram. Soc.*, **54** (1971) 105–12.

23. Knickerbocker, S. H., Zangvil, A. & Brown, S. D., Displacement rate and temperature effects in fracture of a hot-pressed silicon nitride at 1100 to 1325°C. *J. Amer. Ceram. Soc.*, **67** (1984) 365–68.

24. Govila, R. K., Statistical strength evaluation of hot-pressed Si_3N_4. *Amer. Ceram. Soc. Bull.*, **62** (1983) 1251–55, 58.

25. Evans, A. G. & Wiederhorn, S. M., Proof testing of ceramic materials — an analytical basis for failure prediction. *Int. J. Fract.*, **10** (1974) 379–92.

26. Gogotsi, G. A. & Ostrovoy, D. Yu., Deformation behaviour of ceramics in heating. *Refractories*, **33** (1992) 28–34.

27. Gogotsi, G. A., Lomonova, E. E. & Ostrovoy, D. Yu., Deformation behaviour of cubic ZrO_2 single crystals. *Refractories*, **33** (1992) 152–8.

28. Gogotsi, G. A., Deformational behaviour of ceramics. *J. Eur. Ceram. Soc.*, **7** (1991) 87–92.

29. Gogotsi, G. A., Zavada, V. P., Kutnyak, V. V. & Ostrovoy, D. Yu. A machine for determination of the mechanical properties of ceramics at high temperatures. *Strength of Materials*, **20** (1988) 558–62.

30. Gogotsi, G. A. & Swain, M. V., Comparison of strength and fracture toughness of single and polycrystalline zirconia. In *Science and Technology of Zirconia V*, ed. S. P. S. Badwal, M. J. Bannister & R. H. J. Hannink. Technomic Publishing Co., Lancaster, Basel, 1993, pp. 347–59.

31. Rawlins, M. H., Nolan, T. A., Allard, L. E. & Tennery, V. J., Dynamic and static fatigue behavior of sintered silicon nitride: II, Microstructure and failure analysis. *J. Amer. Ceram. Soc.*, **72** (1989) 1338–42.

32. Evans, A. G. & Dalgleish, B. J., Some aspects of the high temperature performance of ceramics and ceramic composites. *Ceram. Eng. Sci. Proc.*, **7** (1986) 1073–94.

33. Davidge, R. W., Briggs A. & Piller, R. C., Limitations to the performance of engineering ceramics under stress at high temperature. *Proc. Brit. Ceram. Soc.*, **39** (1987) 207–14.

34. Gogotsi, G. A., Gogotsi, Yu. G. & Ostrovoy, D. Yu., Mechanical behaviour of hot-pressed boron carbide in various atmospheres. *J. Mater. Sci. Lett.*, **7** (1988) 814–16.

35. Rabotnov, Yu. N. & Milejko, S. T., Short-term creep, Nauka, Moscow, 1970 (in Russian).

36. Belchuk, M., Watt, D. & Dryden, J., Modeling creep in materials with soft boundary phases. *Proc. Int. Symp. Adv. Struct. Mater.*, Montreal, 28–31 Aug., 1988, New York, 1989, pp. 123–9.

37. Clarke, D. R., Perspective concerning grain boundaries in ceramics. *Amer. Ceram. Soc. Bull.*, **69** (1990) 682–5.

38. Cheeseman, C. R. & Groves, G. W., The mechanism of the peak in strength and toughness at elevated temperatures in alumina containing a glass phase. *J. Mater. Sci.*, **20** (1985) 2614–22.